Vol. 19, No. 3 (2020) 1243-1253
Revista Mexicana de Ingeniería Química

Effect of the preparation method on the properties of nanocomposites based on chitosan, montmorillonite and essential oils

Efecto del método de preparación en las propiedades de nanocompositos basados en quitosano, montmorillonita y aceites esenciales

C. A. Romero-Bastida[1]*, G. Velazquez[2], S. Bautista-Baños[1]

[1]*Instituto Politécnico Nacional. Centro de Desarrollo de Productos Bióticos, Carretera Yautepec Jojutla, Km. 6, Calle CeProBi No. 8. Colonia San Isidro, apartado postal 24. Yautepec, Morelos, México. C. P. 62731.*
[2]*Instituto Politécnico Nacional. Centro de Investigación en Ciencia Aplicada y Tecnología Avanzada, Cerro Blanco No. 141. Col. Colinas del Cimatario, Santiago de Querétaro, Querétaro, 76090, México.*

Received: October 15, 2019; Accepted: January, 9, 2020

Abstract

The aim of this study was to know if the addition order of the components in the film forming solution can modify the characteristics of the final film in order to obtain films with improved physical properties intended for packaging applications. Chitosan films (CH) at 1% were elaborated with montmorillonite (MMT) at 10%, essential oils (cinnamon CEO, and thyme TEO) at 1.5% and glycerol. Two methodologies were used: adding MMT at the beginning (M1) or at the end (M2) of the film preparation method. Water vapor permeability (WVP), mechanical properties, solubility (S), x-ray diffraction (XRD), FTIR and contact angle were evaluated. The combined effects of MMT and CEO using M1 produced films with lower WVP and higher tensile strength compared with M2, probably because MMT in M1 had more time in contact with CH than in M2. Also, SEM display a more compact structure in films using M1 with CEO. X-ray diffraction show that films with M1 were exfoliated while with M2 had an intercalated structure. Therefore, CH films with CEO prepared following the M1 process had better properties than those obtained by method 2.

Keywords: Addition order, nanocomposites, montmorillonite, chitosan, essential oils.

Resumen

El propósito de este estudio es el de conocer si el orden de la adición de los componentes en la solución formadora de la película puede modificar sus características para obtener películas con propiedades físicas mejoradas destinadas para el empacado de alimentos. Se elaboraron películas de quitosano (CH) al 1% con montmorillonita (MMT) al 10%, aceites esenciales (canela CEO y tomillo TEO) al 1.5% con glicerol. Se usaron dos metodologías: añadiendo la MMT al principio (M1) o al final (M2) del proceso de elaboración de las películas. Se evaluó la permeabilidad al vapor de agua, (WVP), las propiedades mecánicas, solubilidad (S), difracción de rayos x, FTIR y ángulo de contacto. Los efectos combinados de la MMT y CEO usando M1 produjeron películas con menor WVP y mayor tensión a la factura comparados con M2. Además, SEM presentó una estructura más compacta en las películas usando M1 con CEO. La difracción de rayos X mostró que las películas con M1 estaban exfoliadas mientras que con M2 tenían una estructura intercalada. Por lo tanto, las películas de quitosano con CEO preparadas siguiendo el proceso M1 tienen mejores propiedades que las obtenidas por el proceso 2.

Palabras clave: orden de adición, nanocompositos, montmorillonita, quitosano, aceites esenciales.

1 Introduction

Synthetic petroleum-based polymers have been widely used in a variety of packaging materials; however, because of its poor biodegradability, the waste disposal have resulted in severe environmental pollution. An alternative could be the use of edible or biodegradable packaging materials, with similar properties to those of synthetic materials, to preserve food quality while preventing waste disposal problems. Among the renewable biopolymers used as a raw material to obtain biodegradable films, there are polysaccharides, proteins and lipids, all of them derived from plant or animal sources (Cazón *et al*. 2017).

* *Corresponding author. E-mail*: cbastida@ipn.mx
Tel. (52)55 576000 ext 82509
https://doi.org/10.24275/rmiq/Poly926
issn-e: 2395-8472

One of these biopolymers is chitosan which is obtained from deacetylation of chitin and is capable to form films with high mechanical strength, good adhesion as well as bacterio- and fungi-static properties (Sun *et al*., 2017). Chitosan-based films have moderate oxygen barrier properties and good carbon dioxide barrier properties but, due to their hydrophilic nature, they are susceptible to changes in their functional characteristics due to adsorbed water (Aguirre-Loredo *et al*., 2017).

Many strategies have been followed to improve the barrier and mechanical properties of chitosan-based biodegradable packaging films. One way to reduce water vapor permeability is the use of essential oils (EOs). The hydrophobic nature of essential oils could be exploited to prepare chitosan films with improved barrier against water vapor while preserving the properties of the essential oils (Hafsa *et al*., 2016).

Other way to reduce water vapor permeability is the addition of layered silicates nanoparticles (e.g. sodium montmorillonite) to improve the end-use properties such as barrier and mechanical properties (Abdurrahim, 2019). Usually, the silicate layers in MMT are organized into stacks kept together by van der Waals forces. To obtain polymers with improved properties, it is necessary to break the attractive forces between the layers, thus allowing the polymer to penetrate the clay structure. The final structure will have high tensile properties and low water vapor permeability. Because of their high surface area, clay particles impart unique combination of physical and chemical properties to make these nanocomposites attractive for films and coatings in several industrial processes (Bertolino *et al*., 2016).

Nonetheless, little is known on the effect of changing the order of addition of components in the film formulation process. Although some researchers have used different addition order of film components, Abdollahi *et al*. (2012) used aqueous acetic acid solution of chitosan prepared and mixed with clay solutions, tween and rosemary essential oil. Dias *et al*. (2014), studied solutions containing tocopherol, montmorillonite and chitosan. Lee *et al*. (2018) prepared aqueous solution of chitosan, with glycerol, nanoclay and cinnamon essential oil. These researchers did not investigate the order of aggregation of components. A previous research (Romero-Bastida *et al*., 2015) found that the order of aggregation of MMT and glycerol in starch films can modify the film properties because there is a competition for the active sites in the montmorillonite layers; the first component entering to the clay gallery can modify the final film properties. Therefore, the aim of this study was to evaluate the effect of the order of incorporation of MMT on the properties of chitosan films with essential oils intended for the protection of fruits and vegetables.

2 Materials and methods

2.1 Materials

High-molecular weight chitosan, with a degree of deacetylation of 90% (CH) and sodium montmorillonite (MMT-Na, 682659) were purchased from Sigma Aldrich (USA). Glycerol (G7757) was obtained from Baker (USA), polyoxyethylene monooleate (Tween 80) was obtained from Hycel (México) and essential oils (cinnamon and thyme) were purchased from doTerra (México).

2.2 Film preparation

Films were prepared by dissolving CH in 1% (v/v) aqueous acetic acid solution at 1% (w/v), stirring at 40 °C until complete dissolution. Two methods were used to prepare the films. The difference between the methods was the order in which the components were added. In method 1 (M1), sodium montmorillonite (MMT) at 10% w/v. was subjected to ultrasonic homogenization (Bransonic 1510R_MTH) during 1 h at 80 W, before added to chitosan film solution and stirred for 1 h. Glycerol at 25% (w/v) was added as a plasticizer and tween 80 at 0.2% (w/v) was added as a surfactant. The solution was mixed for 30 min at 40 °C. Cinnamon essential oil (CEO) or thyme essential oil (TEO) were added at 1.5% (v/v). Finally, the solution was homogenized using an Ultra-Turrax homogenizer (T25, Ika-Werke, Germany) at 7000 rpm for 5 min to decrease the drop size of the oils. For film formation, 110 ml of the solution were cast onto acrylic plates (540 cm^2) and dried at 40 °C during 20 h to allow solvent evaporation. Films made by M1 were identified as CH1C or CH1T for cinnamon or thyme essential oil films, respectively. For method 2 (M2), glycerol and Tween 80 were first added to chitosan solution and stirred for 30 min at 40 °C. Then, essential oils were added and homogenized during 5 minutes at 7000 rpm. Next, sonicated MMT was added and stirred for one hour. Lastly, solutions were cast onto acrylic plates and dried as mentioned before. Films made by M2 were identified as CH2C or CH2T

for cinnamon or thyme essential oil films, respectively. The dried films were peeled and stored until further analysis. Control film did not have neither MMT nor essential oils.

2.3 Film characterization

2.3.1 X-ray diffraction (XRD)

The crystalline structure of the chitosan polymer and the MMT clay in the film was determined using a diffractometer (Rigaku, Miniflex 600) with an X-ray tube with Cu radiation Kα(λ= 1.54 A°) with linear focus (40 kV and 15 mA). The scattering 2θ angle ranged from 2 to 40° with a step size of 0.01 at a scanning rate of 4°/min. The basal spacing of the silicate layer (d001) was calculated using the Bragg's diffraction equation: $\lambda = 2\text{d}\ \sin\theta$, where λ is the wavelength of the X-ray diffraction (0.15406 nm), d is the spacing between diffraction lattice planes and θ is the measuring diffraction angle.

2.3.2 Thickness measurement

Thickness was measured using a manual micrometer (Fowler, USA). Measurements were performed at ten random points on the film surface.

2.3.3 Fourier transform infrared spectroscopy (FTIR)

IR spectra were obtained using a IR spectrometer IR (Shimadzu Prestige-21. Kyoto-Japan), equipped with an attenuated total reflectance (Kyoto, Japan) cell. The spectra were recorded in absorbance units and the wave number ranged from 4000 to 400 cm^{-1}. Each sample was scanned 20 times for spectrum integration at a scanning resolution of 2 cm^{-1} using the WinBomem Easy software.

2.3.4 Scanning electron microscopy (SEM)

The morphology of the firms was examined using a scanning electron microscope (JEOL JSM-5410LV. Tokyo, Japan). For the SEM analysis, the samples were cut to an adequate size and placed on a cylindrical copper support (1-cm diameter). The samples were coated with gold to facilitate conduction and prevent the accumulation of charge under electron bombardment. The analysis of the sample was performed under high vacuum conditions.

2.3.5 Water solubility

Water solubility, expressed as percentage, was determined from the dry matter of the film following the method described by García *et al*. (2004). Samples were cut into rectangles (2 x 3 cm), kept in a desiccator with silica gel for 7 days, and weighted. Subsequently, films were immersed in 80 ml of deionized water, kept at 25 °C for one hour under agitation. After this time, the dry matter was determined using an oven at 105 °C until constant weight. Solubility was calculated using Equation 1.

$$Solubility = \frac{M_i - M_f}{M_i} * 100 \quad (1)$$

where M_i is the initial weight and M_f the final weight.

2.3.6 Contact angle

The contact angle was measured using the sessile drop technique with a 5 μl drop of distilled water. The images were obtained with a MicroView 10-800X digital microscope and the ImageJ® software was used to calculate the contact angle.

2.3.7 Mechanical properties

Tensile strength (MPa) and elongation at break (%) of the films were evaluated. Tensile tests were performed using a texture analyzer (TA Plus, Lloyd Instruments). Rectangular samples (100x10 mm) were cut from the films according to the ASTM method D882-02. Film samples were conditioned at 57% RH for 72 h before testing. The initial distance between grips was 60 mm and the cross-head speed was 1 mm/s. Al least 10 samples were measured for each film. Tensile strength (TS) was calculated dividing the maximum peak force by the initial cross-section area of the film. Similarly, the percentage of elongation (%E) was calculated dividing the change in length at the break point by the initial length of the film times 100.

2.3.8 Water vapor permeability (WVP)

WVP test was conducted following the ASTM E96-66 method. Films were conditioned at 57% RH for 72 h before testing. A stainless-steel cup (55 mm height and 65 mm in diameter) was used as a permeability device. Each film was sealed over a circular opening of the cup containing a saturated solution of NaCl (75% RH). The permeability cell sealed with the film was placed on the plate of the analytical balance inside a permeability chamber containing silica gel

(0% RH). The cup allowed a transfer area of 53 mm in diameter and the temperature in the whole chamber was controlled at 30±0.5 °C. Data was automatically recorded every 30 min during 6 h. The water vapor transfer was determined from the weight loss of the permeation cup as a function of time. The coefficient of the straight line, obtained by linear regression, was considered as the flux of water vapor. Water vapor transmission rate (WVTR) was calculated dividing the flux by the transfer area. The water vapor permeability was calculated dividing the WVTR by the difference of water vapor pressure in both sides of the film times the thickness of the material. All tests were conducted in triplicate.

2.3.9 *Statistical analysis*

Results are expressed as mean ± standard deviation (SD). Differences between samples were analyzed using analysis of variance (ANOVA) with Sigma STAT. Where significant differences were present, a Tukey pairwise comparison of the means was conducted to identify where the sample differences occurred ($P < 0.05$).

3 Results and discussion

3.1 *X-Ray diffraction*

The XRD patterns of the MMT and the nanocomposites are shown in Figure 1. Peaks represent inter-layer spacing values yielding information about the morphology of the analyzed material.

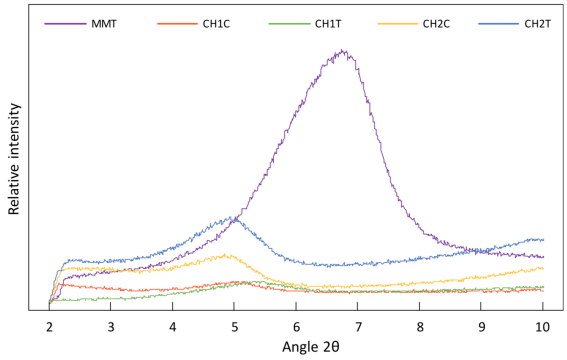

Fig. 1. XRD patterns of montmorillonite and chitosan nanocomposites prepared following two methods using essential oils.

Characteristic peaks of pristine MMT (2θ= 6.91°) are shifted to different angles in the films prepared following the method 2 (CH2C 2θ=4.86° and CH2T 2θ= 4.98°). This behavior could indicate that polymer chains of the chitosan penetrated between the clay layers and forced apart the platelets, thus increasing the gallery spacing. The distance d001 of pure clay (1.28 nm) is typical of hydrated Na-montmorillonite and it is lower than the distance observed in the peaks of nanocomposites made from CH2C and CH2T (1.81 and 1.77 nm, respectively), indicating an intercalated nanocomposite as mentioned by other researchers (Xu *et al*., 2006; Tang *et al*., 2009). Heydari *et al*. (2013) studied nanocomposites formed with starch/glycerol/ MMT and mentioned that obtaining partially or fully exfoliated nanocomposites depends on formulations and methods of film preparation. A broad peak was observed in films prepared following the method 1 (CH1C, CH1T); this could indicate a partial delamination of the clay resulting in an exfoliated structure. Besides, in method 1, chitosan was in contact only with montmorillonite for one hour, enough time to enter the gallery, open the structure and promote its delamination. On the other hand, in method 2, chitosan and glycerol were added at the same time and it is not clear which one of the two compounds reached a better interaction with MMT and how the clay galleries could have been modified. According to Chen and Evans (2005), many polymers, when uptaken by MMT, produce an expanded structure with d001 values of about 1.8 nm. Similar results were observed in the present study when the method 2 was used, suggesting that there is a competition for active sites in MMT. The adsorption and intercalation of glycerol into clay galleries is well known and it has been studied for many years (Tang *et al*., 2008). In fact, glycerol used as a plasticizer in method 2, could have prevented the entry of chitosan molecules into the lamellar spaces of MMT and may have covered the entire inter-layer space.

3.2 *FTIR analysis*

FTIR was used to investigate the changes in chitosan films structure on a short-range molecular level and to identify the potential interactions among the components. Figure 2a shows typical chitosan FTIR spectrum that has been reported with bands corresponding to distinct functional groups. All spectra exhibited the characteristic two strong bands of the amide groups at 1564 and 1417 cm^{-1} ascribed respectively to the C=O stretching and NH bending

modes (Wang *et al*., 2005).

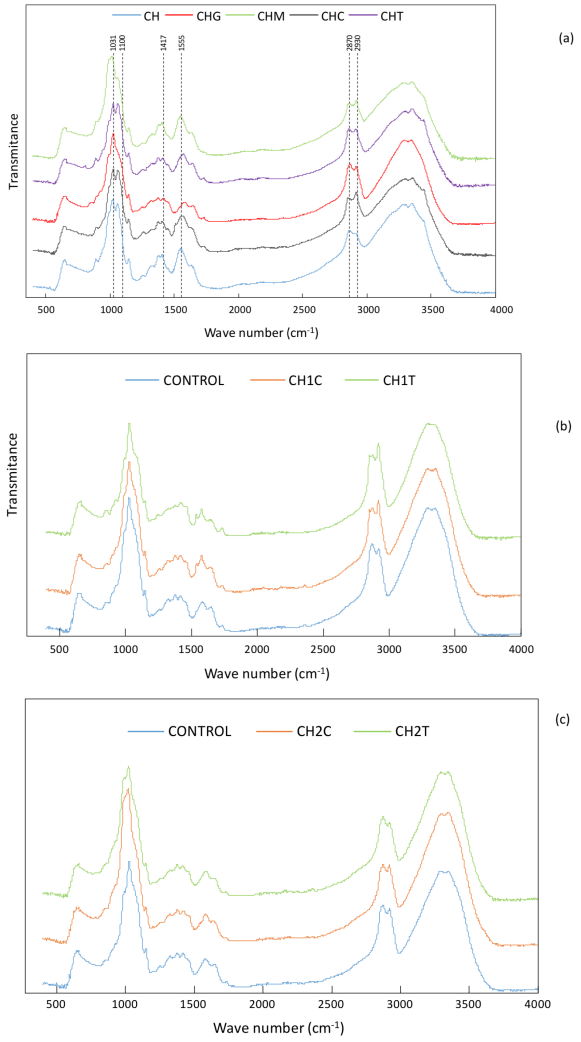

Fig. 2. FTIR spectra of chitosan film (CH), chitosan/glycerol film(CHG), chitosan/MMT film (CHM), chitosan/cinnamon essential oil film (CHC) or chitosan/ thyme essential oil (CHT) (a), and its nanocomposites made by method 1 (b) and method 2 (c).

The shoulder at approximately 1555 cm^{-1} in films with no added glycerol (CH), is assigned to the-NH_3^+ $-OOCCH_3$ interactions. An indicator for interaction between chitosan film with glycerol could be seen at 2847 cm^{-1} that could be due to stretching of C-H (Devandi *et al*., 2016). The bands appearing at 2930 and 2870 cm^{-1} in the spectrum of CH film are due to stretching vibrations of the C-H bond in CH_2 and CH_3 groups, respectively, as mentioned by Abdolahi *et al*. (2012). These peaks became sharper when essential oils were added, especially when CEO was added (CHC in the Figure 2a) indicating a strong interaction between CEO and chitosan. This behavior may be due to a formation of a linkage between phenolic compounds present in the essential oils and chitosan. This behavior was also reported by Shen and Kamdem (2015) for chitosan film with citronella essential oil and cedar wood oil.

For chitosan-MMT films, absorption bands of adsorbed molecular water appeared at 1630 and 3400 cm^{-1}. The broad band found at 3100 cm^{-1} is due to overlapped -OH, MMT and -NH groups in chitosan. The signal observed at 2900 cm^{-1} is attributed to C-H bands. The CH film exhibited a strong absorption band between 3000 and 3500 cm^{-1} that corresponded mainly to the stretching vibration of free hydroxyl and to the asymmetric and symmetric stretching of the N-H bonds. In this study, FTIR spectra of films prepared following the both methods (Figure 2b, 2c) have little differences only that the double peak in the range of 1000 cm^{-1} became one.

3.3 Film microstructure

Figure 3 shows SEM images of the surface and cross-section of chitosan and chitosan-based nanocomposite films. The structure of pure chitosan films was compact and the surface was smooth with no pores or cracks (Figure 3a). When MMT and CEO were added, the films showed a rougher surface (Figure 3c). Also, cinnamon essential oil appears to be more compatible with the chitosan matrix than the thyme oil (Figure 3b). Similar behavior was reported by Wang *et al*. (2011), who studied chitosan films added with cinnamon and clove bud oil. The authors found that films added with clove oil exhibited a phase separation but films containing cinnamon essential oil showed a uniform structure. The cross section of chitosan films with cinnamon essential oil revealed the sheets stacked in compact layers (Figure 3d), showing small droplets of CEO incorporated uniformly into the matrix. With these results it could be expected a low WVP values of films elaborated with MMT and CEO following the method 1. Hoseini *et al*. (2009) mentioned that the incorporation of essential oils into chitosan films resulted in a loss in the compactness of the structure, and this effect is more accused with cinnamon essential oil in comparison with thyme and clove oils. However, in the current study, chitosan films with MMT and TEO (Figure 3f) exhibited a less compact structure than chitosan films added with MMT and CEO (Figure 3d), probably because of the incorporation of MMT into the formulation.

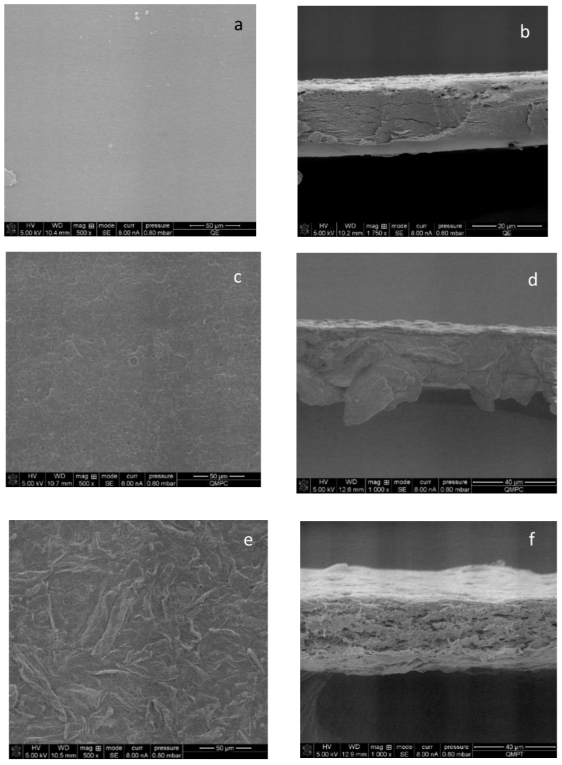

Fig. 3. Scanning electron microscopy images of surface and cross-section respectively: chitosan control film, (a, b) chitosan film with cinnamon essential oil (c, d) and chitosan film with thyme oil (e, f) using method 1.

3.4 Solubility

Solubility is a very important film property that measures the resistance to water. Figure 4 shows the solubility percentages of composite films added with EO.

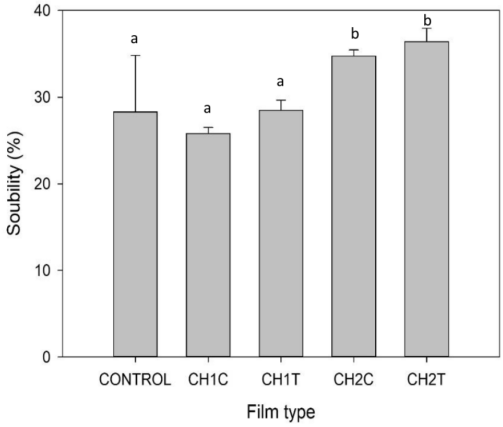

Fig. 4. Solubility of chitosan film nanocomposites with essential oils made by two methodologies.

A decreasing in solubility was observed when cinnamon essential oil was used (CEO). Similar results have been reported by Ojagh *et al*. (2010) for chitosan films incorporated with CEO. The authors explained that CEO formed covalent bonds between the functional groups of chitosan chains decreasing the availability of hydroxyl and amino groups to form hydrogen bonds with water molecules. Other researchers indicated that a high cross-linking of chitosan chains with essential oils leads to a matrix with low affinity to water (Adbollahi *et al*. 2012). Solubility reduction of films incorporated with EOs could be due to an increase in the hydrophobic nature and influenced by the loss of free functional groups (amino and hydroxyl). The low water affinity of films added with the two EOs is important for their application as a coat in food products with high moisture contents like fresh fruits. Also, the incorporation of MMT into the chitosan film significantly decreased ($p < 0.05$) the solubility values only when method 1 was used. The solubility of control film (33%) in this study is lower than the 40% value reported by López-Mata *et al*. (2015). The solubility values for chitosan films obtained using method 1 (24%) were lower than those found by Nuñez-Gastelum *et al*. (2019) using moringa oil extract (33%), maybe because in this study there was a combination of essential oils and montmorillonite.

Differences in results could be due to differences in chitosan properties, which vary depending on the source, deacetylation degree, and molecular weight. Moreover, solubility could also be influenced by the presence of the plasticizer used during the film preparation process and the functional groups in the chitosan chains (Park *et al*., 2002).

3.5 Contact angle

Contact angle is defined as the angle between the substrate surface and the tangent line at the point of contact of the liquid droplet with the substrate. The contact angle is a good indicator of the relative hydrophobicity or hydrophilicity of a substrate (Rivero *et al*., 2012). When a water droplet is placed on a polymer surface, an attraction occurs between the molecules in the water and the polymer surface. The strength of the attraction depends on the properties of the solid. A lower contact angle between the polymer and water means that they have a strong attraction; therefore, water adhere better to the polymer (Handojo *et al*., 2009).

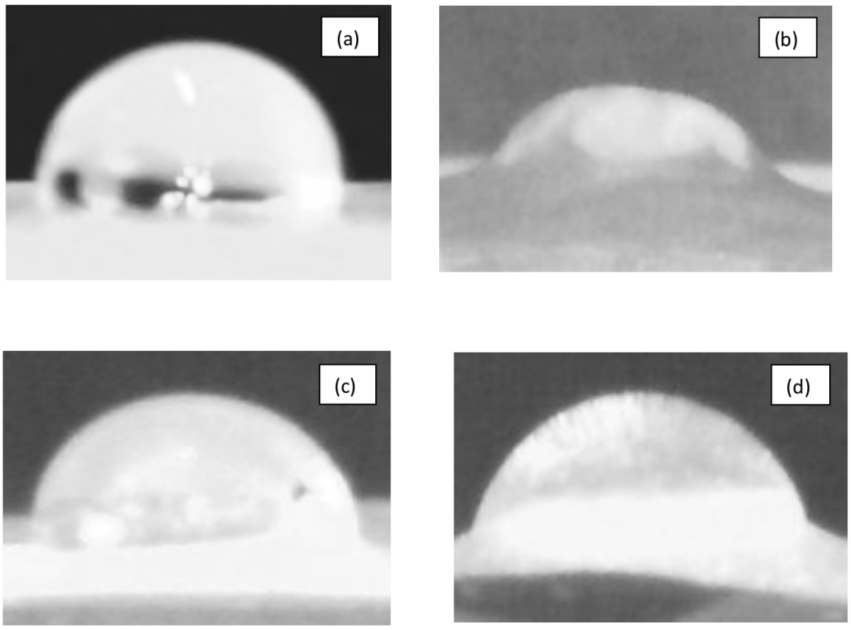

Fig. 5. Photograph of a drop of water in the surface of chitosan films elaborated with (a) MMT, (b) glycerol, (c) MMT, glycerol and cinnamon essential oil using method 1(CH1C), (d) MMT, glycerol, and cinnamon essential oil using method 2(CH2C).

Although chitosan film is a hydrophilic material, its wettability could be affected when blended with other material. Heydari *et al*. (2013) measured contact angle in cornstarch films and concluded that by changing the filmogenic formulation, contact angle varies when using glycerol or MMT. In this study, contact angle decreased when using glycerol (Figure 5b). It means that the presence of glycerol increased the hydrophilicity of the film. Adding Na-MMT into the formulation (Figure 5a), the surface of the biopolymer became hydrophobic and the contact angle increased. Similar behavior was observed with CH films when using glycerol or MMT showing contact angle values of 32.4° and 66.5° for glycerol and MMT, respectively. The behavior observed in the solubility test are confirmed with the wettability of films using method M1 (Figure 5c) and method M2 (Figure 5d). Contact angles were 61.47° and 47.04° for M1 and M2, respectively. In this way, the sequence of the component addition had an important effect on the hydrophilicity of films because in method M1 chitosan is first interacting with MMT then glycerol and finally with the essential oils. In method M2 chitosan interacted first with the glycerol and the behavior is driven by the hydrophilic properties of glycerol. In a previous study, (Romero-Bastida *et al*., 2015) the authors hypothesized a competition for active sites between the polymer and the clay that resulted in different film properties depending of the adding order.

3.6 Mechanical properties

Mechanical properties data of chitosan and nanocomposites are shown in Figure 6. Results have a high standard deviation but still, statistical differences between treatments were detected. This could be explained by the way the samples were cut or maybe because there was some heterogeneity in the films. Results indicate that TS (Figure 6a) increased significantly by incorporating MMT and CEO into the formulation of films prepared following the method 1. This behavior could be explained because cinnamon essential oil is more compatible with chitosan than thyme essential oil, as a more homogeneous structure was observed in SEM images. These results are in agreement with those reported by Ojagh *et al*. (2010), who found that incorporating CEO into chitosan films increased tensile strength values significantly ($p < 0.05$). The authors mentioned that a strong interaction between the polymer and the CEO resulted in a cross-linking effect, which decreased the free volume and the molecular mobility of the polymer observed as a compact structure in SEM photographs.

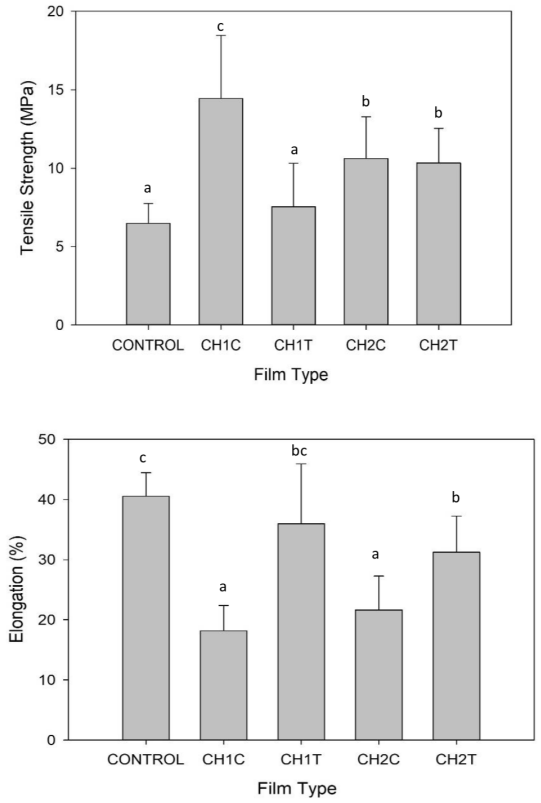

Fig. 6. Mechanical properties of chitosan film and its nanocomposites using two methods.

Hosseini *et al*. (2009), found that chitosan films incorporated with thyme essential oil showed a loose texture similar to a sponge-like structure. They postulated that the loose structure observed in these films may be caused by the thyme essential oil components disrupting the ordered structure of the chitosan polymers explaining the lower tensile strength values of this films when compared to films with CEO. Peng and Li (2014), investigated the physical and mechanical properties of chitosan films with different essential oils: thyme, cinnamon, lemon and their combinations. The authors mentioned that the interactions in the matrix varied with each kind of EOs. Moreover, the chitosan composition, plasticizer presence and the emulsification method also had an important effect on the mechanical properties of the films, thus resulting in the variation in mechanical properties, having the best results when CEO was used. Although MMT promoted a rougher structure when method 1 was used, the surface of the film was smoother than the one that used method 2. It means that a better dispersion of MMT (and CEO) in the matrix occur and resulted in enhanced mechanical properties. The exfoliation morphology of MMT in method 1 (as seen in XRD) provides a better reinforcement in the structure that caused greater tensile strength. Similar results (T= 20 MPa) was found with other nanoparticles like titanium dioxide in chitosan films to reinforce their structure as those found by Gonzalez-Calderón *et al*. (2019). The high values in %E (Figure 6b) observed in chitosan films with TEO using method 2 may be explained by a more open structure shown in SEM images. Differences in methods can also be appreciated in film thickness as values of 0.042 and 0.043 mm were obtained for CH1C and CH1T, respectively, prepared following the method 1; meanwhile, thickness of 0.065 and 0.062 mm were obtained for CH2C and CH2T, respectively, using the method 2. Thickness results indicate a more compact or a wider structure for M1 or M2, respectively.

3.7 Water vapor permeability

Water vapor permeability indicates the rate at which water molecules are transferred through the film. The WVP values of chitosan and chitosan-based nanocomposite films are shown in Figure 7. The lowest values were found in films prepared following the method 1. The inclusion of MMT and EOs decreased WVP by 32% compared with control films. The results obtained in this study for films with cinnamon oil and MMT (4.5 X 10^{-11} g/m s Pa) are lower than those reported by Ojagh *et al*. (2010) when using cinnamon oil in chitosan films (10.1 X 10^{-11} g/m s Pa). Probably because they used only essential oils in the film and in the current study, a synergic effect of clay and EO could have taken place.

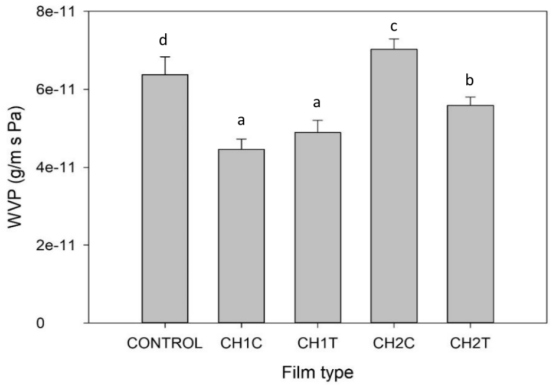

Fig. 7. Water vapor permeability of chitosan and chitosan nanocomposite films using two preparation methods.

Essential oils might increase the hydrophobic character of the film and, on the other hand, the presence of ordered dispersed clay layers decreased WVP by creating a tortuous path through the polymer matrix (Rhrim *et al*., 2006; Tang *et al*., 2009). This behavior is similar to that reported by Abdollahi *et al*. (2012) for films based on chitosan, MMT and rosemary essential oil. Other researchers indicate that the hydrogen and covalent bonds between the chitosan chains and EO molecules could limit the amount of groups available to form hydrogen bonds with water decreasing WVP values (Siripatrawan and Harte, 2010). The low values of WVP agrees with the results found in mechanical properties in which a higher tensile strength was found when using method 1. Conversely, higher values of WVP of films made with method 2 agrees with higher values of elongation because of a more open structure found in SEM.

In this study, although the films have the same components, the preparation method 1 allowed obtaining the lowest WVP values mainly because MMT was added first favoring a strong interaction with the polymer. This hypothesis was supported by FTIR spectra showing the interaction of chitosan functional groups with MMT in the presence of EO.

Conclusions

The addition of MMT and cinnamon essential oil to chitosan films led to significant changes in their physical and mechanical properties. The results showed a unique compatibility achieved between chitosan and CEO which caused a significant decrease in WVP and solubility as well as an increase in tensile strength when the method 1 was used. The improvement of these properties could be reflected in a compact structure, as demonstrated by SEM in films with cinnamon essential oil in contrast with the sponge-like structure found in films with thyme essential oil. Also, cinnamon essential oil provided a more hydrophobic surface evidenced by a higher contact angle. MMT also improved the effect of cinnamon essential oil by having and exfoliated morphology when using the method 1 instead of an intercalation morphology when using the method 2. Finally, FTIR spectra demonstrated an interaction between chitosan and the added compounds.

Acknowledgements

We appreciate the financial support from EDI-IPN, and to Dra. Maraolina Domínguez Díaz and Dr. Bernardo Campillo Illanes of Laboratorio de Espectroscopia ICF-UNAM for the technical assistance in measuring contact angle. Also, the experimental support of the CNMN-IPN for the realization of XRD and FTIR in this research.

References

Abdollahi, M., Rezaei M., Farzi, G. (2012) A novel active bionanocomposite Film incorporating rosemary essential oil and nanoclay into chitosan. *Journal of Food Engineering 111*, 343-350. https://doi.org/10.1016/j.jfoodeng.2012.02.012

Abdurrahim, K. I. (2019) Water sorption, antimicrobial activity, and thermal and mechanical properties of chitosan/clay/glycerol nanocomposite films. *Heliyon 5*, e02342. https://doi.org/10.1016/j.heliyon.2019.e02342

Aguirre-Loredo, R. Y., Rodriguez-Hernandez, A. I., Velazquez, G. (2017). Modelling the effect of temperature on the water sorption isotherms of chitosan films. *Food Science and Technology, Campinas 37*, 112-118. http://dx.doi.org/10.1590/1678-457x.09416

Bertolino, V., Cavallaro, G., Lazzara, G., Merli, M., Miloto, S., Parisi, F. Sciascia, L. (2016). Effect of the biopolymer charge and the nanoclay morphology on nanocomposite materials. *Industrial & Engineering Chemistry Research 55*, 7373-7380. https://doi.org/10.1021/acs.iecr.6b01816

Cazón, P., Velázquez, G., Ramírez, J. A., Vázquez, M. (2017). Polysaccharide-based films and coatings for food packaging: A review. Food Hydrocolloids 68, 136-148. https://doi.org/10.1016/j.foodhyd.2016.09.009

Chen, B. and Evans, J.R.G. (2005). thermoplastic starch-clay nanocomposites and their characteristics. *Carbohydrate Polymers 61*, 455-463. https://doi.org/10.1016/j.carbpol.2005.06.020

Devandi, M. V., Bernal, C., Francois, N. J. (2016). Development of biodegradable films based on chitosan/glycerol blends suitable for medical applications. *Journal of Tissue Engineering 7*, 87-196. https://doi.org/10.4172/2157-7552.1000187

Dias, M. V., Machado Azevedo, V., Borges, S. V., Soares, N. D. F. F., de Barros Fernandes, R. V., Marques, J. J. Medeiros, É. A. A. (2014). Development of chitosan/montmorillonite nanocomposites with encapsulated α-tocopherol. *Food Chemistry 165*, 323-329. https://doi.org/10.1016/j.foodchem.2014.05.120

Ding, E. Q. Wu, C. Liang (2011). Discrimination of cinnamon bark and cinnamon twig samples sourced from various countries using HPLC-based fingerprint analysis. *Food Chemistry 127*, 755-760. https://doi.org/10.1016/j.foodchem.2011.01.011

García, A., Pinottia, A., Martinoa M. N., and Zaritzkya, N. E. (2004). Characterization of composite hydrocolloid films. *Carbohydrate Polymers 56*, 339-345. https://doi.org/10.1016/j.carbpol.2004.03.003

Giatrakou, V., Ntzimani, A., Savvaidis, I. (2010). Effect of chitosan and thyme oil on a ready to cook chicken product. *Food Microbiology 27*, 132-136. https://doi.org/10.1016/j.fm.2009.09.005

Gonzalez-Calderon, J. A., Vallejo-Montesinos, J., Martínez-Martínez, H. N., Cerecero-Enríquez, R., & López-Zamora, L. (2019). Efecto de la modificación química de las partículas de dióxido de titanio mediante silanización sobre las propiedades de las películas de chitosan/almidón de papa. *Revista Mexicana de Ingeniería Química 18*, 913-927. https://doi.org/10.24275/uam/izt/dcbi/revmexingquim/2019v18n3/GonzalezC

Hafsa, J., Smach, M., Khedher, M. R. B., Charfeddine, B., Limem, K., Majdoub, H., and Rouatbi, S. (2016). Physical, antioxidant and antimicrobial properties of chitosan films. *LWT - Food Science and Technology 68*, 356e364. https://doi.org/10.1016/j.lwt.2015.12.050

Heidari, A., Alemzadeh, I., and Vossoughi, M. (2013). Functional properties of biodegradable corn starch nanocomposites for food packaging applications. *Materials and Design.50*, 954-961. https://doi.org/10.1016/j.matdes.2013.03.084

Hosseini, M., Razavi, S., and Mousavi, M. (2009). Antimicrobial, physical and mechanical properties of chitosan-based films incorporated with thyme, clove and cinnamon essential oils. *Journal of Food Process and Preservation 33*, 727-743. https://doi.org/10.1111/j.1745-4549.2008.00307.x

Lee, M. H., Kim, S. Y. and Park, H. J. (2018). Effect of halloysite nanoclay on the physical, mechanical, and antioxidantproperties of chitosan films incorporated with clove essential oil. *Food Hydrocolloids 84*, 58-67. https://doi.org/10.1016/j.foodhyd.2018.05.048

Lopez-Mata, M.A., Ruiz-Cruz, S., Silva-Beltrán, N.P., Ornelas-Paz, J.D., Zamudio-Flores, P.B., and Burruel-Ibarra, S.E. (2013). Physicochemical, antimicrobial and antioxidant properties of chitosan films incorporated with carvacrol. *Molecules 18*, 13735-13753. https://doi.org/10.3390/molecules181113735

Núñez-Gastélum, J. A., Rodríguez-Núñez, J. R., de la Rosa, L. A., Díaz-Sánchez, A. G., Alvarez-Parrilla, E., Martínez-Martínez, A., and Villa-Lerma, G. (2019). Análisis de las propiedades físicas y estructurales de las películas de quitosano-policaprolactona adicionadas con extracto de hoja de moringa oleífera. *Revista Mexicana de Ingeniería Química 18*, 99-106. https://doi.org/10.24275/uam/izt/dcbi/revmexingquim/2019v18n1/Nunez

Ojagh, S., Rezaei, M., Razavi, S. and Hosseini, S. (2010). Effect of chitosan coatings enriched with cinnamon oil on the quality of refrigerated rainbow trout. *Food Chemistry 120*, 193-198. https://doi.org/10.1016/j.foodchem.2009.10.006

Park, S.Y., Marsh, K.S. and Rhim, J.W. (2002). Characteristics of different molecular weight chitosan films affected by the type of organic solvents. *Journal of Food Science 67*, 194-197 https://doi.org/10.1111/j.1365-2621.2002.tb11382.x

Peng, Y., and Li, Y. (2014). Combined effects of two kinds of essential oils on physical, mechanical and structural properties of chitosan films. *Food Hydrocolloids 36*, 287e293 https://doi.org/10.1016/j.foodhyd.2013.10.013

Rivero, S., García, M.A., and Pinotti, A. (2012). Heat treatment to modify the structural and physical properties of chitosan-based films. *Journal of Agricultural and Food Chemistry 60*, 492-499. https://doi.org/10.1021/jf204077k

Rhim, J. W., Hong, S. I., Par k, H. M., and Ng, P. K. W. (2006). Preparation and characterization of chitosan-based nanocomposite films with antimicrobial activity. *Journal of Agricultural and Food Chemistry 54*, 5814-5822. https://doi.org/10.1021/jf060658h

Romero-Bastida, C.A., Bello-Pérez, L. A., Velázquez, G., and Alvarez-Ramirez, J. (2015). Effect of the addition order and amylose content on mechanical, barrier and structural properties of films made with starch and montmorillonite. *Carbohydrate Polymers. 127*, 195-201. https://doi.org/10.1016/j.carbpol.2015.03.074

Siripatrawan, U. and Harte, B.R. (2010). Physical properties and antioxidant activity of an active film from chitosan incorporated with green tea extract. *Food Hydrocolloids 24*, 770-775. https://doi.org/10.1016/j.foodhyd.2010.04.003

Shen, Z., and Kamdem, D. P. (2015). Development and characterization of biodegradable chitosan films containing two essential oils. Inter. *Journal of Biological Macromolecules 74*, 289-296. https://doi.org/10.1016/j.ijbiomac.2014.11.046

Sun, L., Sun, J., Chen, L., Niu, P., Yang, X., and Guo, Y. (2017). Preparation and characterization of chitosan film incorporated with thinned young apple polyphenols as an active packaging material. *Carbohydrate Polymers 163*, 81-91. https://doi.org/10.1016/j.carbpol.2017.01.016

Tang, C., Chen, N., Zhang, Q., Wang, K., Fu, Q., and Zhang, X. (2009). Preparation and properties of chitosan nanocomposites with nanofillers of different dimensions. *Polymer Degradation and Stability 94*, 124-131. https://doi.org/10.1016/j.polymdegradstab.2008.09.008

Tang, X., Alavi, S. and Herald, T. J. (2008). Effects of plasticizers on the structure and properties of starch-clay nanocomposite films. *Carbohydrate Polymers 74*, 552-558. https://doi.org/10.1016/j.carbpol.2008.04.022

Wang, L., Liu, F. Jiang, Y., Chai, Z. Li, P. Cheng, Y. Jing, H., and Leng, X. (2011). Synergistic antimicrobial activities of natural essential oils with chitosan films. *Journal of Agricultural and Food Chemistry 59*, 12411-12419. https://doi.org/10.1021/jf203165k

Wang, S., Shen, L., and Tong, Y. (2005). Biopolymer chitosan/montmorillonite nanocomposites: preparation and characterization. *Polymer Degradation and Stability 90*, 123-131. https://doi.org/10.1016/j.polymdegradstab.2005.03.001

Xu, Y., Ren., X., and Hanna, M. A. (2006). Chitosan/clay nanocomposite film preparation and characterization. *Journal of Applied and Polymer Science 99*, 1684-1691. https://doi.org/10.1002/app.22664